

Self-Assembled Nanobiomaterials

Steve S. Santoso and Shuguang Zhang

*Center for Biomedical Engineering and Department of Biology,
Massachusetts Institute of Technology, Cambridge, Massachusetts, USA*

CONTENTS

1. Introduction
 2. Peptide Systems
 3. Nucleic Acid Systems
 4. Lipid System
 5. Biological Selection of Peptides
 6. Summary
- Glossary
Acknowledgments
References

1. INTRODUCTION

Human history has been famously subdivided into distinct ages of materials. Indeed, the progress of scientific sophistication has been tightly linked to the nature of the materials that were predominant in the different eras. The Stone Age, for example, represented the earliest of human ingenuity, when our primitive ancestors created and improved simple tools out of natural rocks. Subsequent Bronze and Iron Ages revealed increased technological savvy as tools and equipments were made from extracted and processed materials. In the "Plastic Age," mankind perfected the science of organic synthesis; and recently, the "Silicon Age" has yielded unprecedented progress in extremely complex electrical devices. In the future, each of these materials will most likely occupy its own niche such that no new material will completely render the previous ones obsolete. However, it can be argued that further progress in particular fields such as regenerative medicine [1], engineering [2, 3], and recently nanotechnology [4] will benefit tremendously from the discovery and development of novel, designed, and integrated materials.

Throughout these ages, scientists have searched for lighter, stronger, more energy-efficient, and in recent times, smaller materials. Materials found in nature in these respects have continued to awe us with their versatility and superiority. The spider silk microfiber, for example, is tougher than steel or Kevlar [5] per unit weight. The

male moth antenna can detect a single pheromone molecule secreted by a female over great distances [6], putting current biosensing technology to shame. Breakthroughs in molecular biology and biophysics are starting to give us a glimpse of the molecular basis for these behaviors, and we are starting to learn the basic rules for the organization of biological macromolecules such as proteins, deoxyribonucleic acids (DNA), and ribonucleic acids (RNA) that confer such phenomenal attributes.

Biologists and material scientists are not only interested in the scientific underlying of these natural materials but also in their mimicry and utilization for different applications [7]. Even though spider silk or a moth antenna is currently too difficult to mimic, we have come to realize that biological materials, in general, may have superior qualities over man-made ones for certain applications. Furthermore, any research into biomaterials has benefited from decades of improvements in the chemical synthesis methods of biopolymers, not to mention a wealth of data generated from basic research. Designed peptide molecules, for example, can be synthesized rapidly and analyzed using standard techniques for studying protein structure such as circular dichroism, electron microscopy (EM), and nuclear magnetic resonance (NMR).

A subset of biological materials is the subject of this entry, and all of the members of this set share the same enabling property: they are formed through the self-assembly of particular motifs of biological polymers. Spontaneous associations of diverse molecules into a distinct supramolecular assembly is ubiquitous in biology: for example, the eubacterial ribosome consists of more than 50 proteins and three ribosomal ribonucleic acid molecules that self-organize into a molecular machinery which can perform complex reactions that synthesize proteins [8]. Such nanoscale organizations occur without human instructions or interference, resulting in the formation of structures with little energy expenditure [9].

We will first present the case of self-assembling peptides and describe how researchers have used these systems to create different materials for applications such as mineralization, formation of nanowires, anti-microbial agents, and growth of tissues. We will then focus on DNA molecules

that have been utilized as templates for metallization and engineered to form crystalline structures. Last, we will summarize the use of larger biological entities: bacterial viruses that allow inorganic metal ions to self-assemble on their surfaces. While practically all of these materials are still in their infancy, the promise of biologically inspired materials has galvanized some researchers to study and improve them vigorously. It is our hope that this entry will show the vast promise that biologically inspired materials have on the advancement of many nano-engineering and medical disciplines.

2. PEPTIDE SYSTEMS

2.1. Introduction to Peptides

Peptides and proteins are biopolymers that are the workhorses of the cell. Their functions are as various as their structures, most playing the roles of enzymes that accelerate reaction rates, membrane proteins that act as channels and molecular transporters, while others act as the structural components which enable a cell to hold its shape and to move about. Each is a polymer that is made up of a linear combination of amino acids (Figures 1A and 1B) and can vary in length between a few to tens of amino acids (also called “residues” in the vernacular of biology) in the case of signaling peptides to ten thousand long in a membrane protein of a human cell [10]. This structural versatility of proteins is afforded by the vastness of the amino acid alphabet.

There are 20 naturally occurring amino acids to choose from so that for a 10-amino-acid-long peptide, nature has the option of making 20 [10] (approximately 10 trillion) different species. The peptides and proteins that are found in nature, however, have been selected through billions of years of evolution so that what is left is a miniscule subset of all the possible sequences. These are the proteins whose amino acid sequences give distinct three-dimensional structures or folds so that they can perform tasks in an extremely specific and efficient manner. Indeed, the structure of a protein is the chief reason for its function, and it has been the holy grail of structural biology to predict the three-dimensional structure of a protein from its amino acid sequence.

In essence, biomaterial and nanoscale scientists want to do just the reverse: knowing a desired structure, can he or she design a sequence that can self-assemble to form it? Even though our knowledge of how linear protein molecules

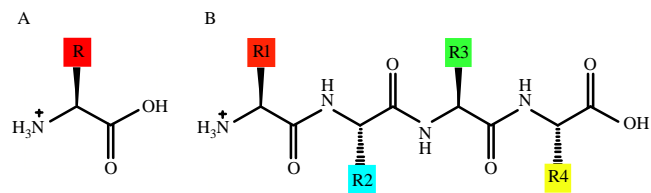


Figure 1. (A) Chemical structure of an amino acid. The side chain, labeled “R” here, can be any one of the 20 naturally occurring amino acids or their derivatives; (B) a four residue (amino acid) peptide. Each peptide is covalently linked to the adjacent one through a peptide amide bond.

fold into higher order structures is still rather rudimentary, the basic principles that we have learned so far have enabled researchers in biological materials to design peptide systems which have already shown considerable promise for a broad range of applications.

2.2. Peptides That Self-Assemble Into Fibers for Biomineralization

Hartgerink et al. reported the rational design [11] and application of a peptide-amphiphilic molecule in a biomineralization process that is akin to the collagen fibers in bone tissue [12]. This lowest structural level in bone is already rather complex, since it involves the integration of an organic protein component with an inorganic, hydroxyapatite (HA) crystal component. Furthermore, the crystals grow in a particular orientation within the collagen fibrils, with their unit cell *c* axis parallel to the long axis of the fibrils [13]. Certainly, any biomaterial that has the potential to replace bone tissue at this level must have similar properties.

Hartgerink et al. synthesized a peptide molecule with a 16-carbon alkyl tail (Figure 2A). The hydrophobicity of the tail and the conical shape of the polymer would drive the self-assembly into cylindrical micelles [14] (Figure 2B). The peptide itself contained amino acids that were deemed to be crucial for particular functions: a string of cysteine residues following the alkyl chain would form intermolecular disulfide bridges, which would confer structural integrity for the self-assembled nanofibers; a linker group made up of glycine residues provided structural flexibility; a phosphoserine residue promoted the nucleation of HA crystals; and an

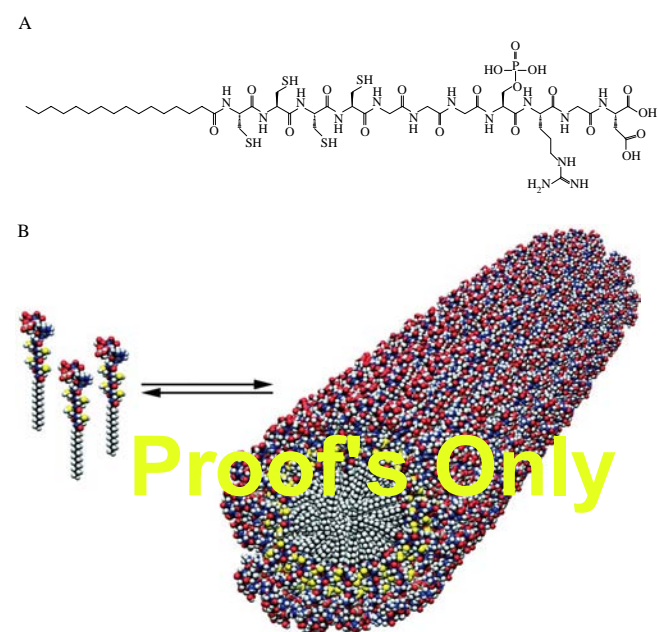


Figure 2. (A) Peptide amphiphile synthesized by Hartgerink et al. for use in biomineralization of hydroxyapatite crystals [11, 12]; (B) the self-assembly of this peptide amphiphile molecule into a cylindrical micelle. The peptide is diagrammed as a van der Waals space-filling model. Reprinted with permission from [12], J. D. Hartgerink et al., *Science* 294, 1684 (2001). (©) 2001, American Association for the Advancement of Science.

RGD sequence motif, which capped the peptide, promoted cell adhesion.

They discovered the assembly of cylindrical micelles under acidic conditions and disassembly in alkaline ones. Cross-linking of the cysteine residues through air oxidation further stabilized the assembled nanostructures. The ability to assemble or disassemble supramolecular assemblies selectively under controlled conditions is beneficial when making new materials since it allows for reversibility of any undesired structures. Further experiments also revealed that the nanofibers have the potential to nucleate HA crystals in the correct orientation. This promising result highlighted the possibility of using biomolecules or their derivatives in making novel materials for medicine and tissue repair and regeneration.

2.3. Peptides That Form Tubes and Vesicles

2.3.1. Short Amphiphilic Peptides

Ideally, the biopolymer constituents used for self-assembly into materials should be rather inexpensive to synthesize in large quantities, easy to handle, and chemically uncomplicated so analysis and modeling can be performed with a reasonable amount of effort. Our laboratory has designed a simple peptide system having those properties [15, 16]. We made short peptides of around six to seven amino acids that had the properties of surfactant molecules in that each monomer contained a polar and a nonpolar region. For example, a peptide called A_6D had six hydrophobic alanine amino acids followed by one polar, negatively charged aspartic acid (Figure 3A). In essence, the molecule looked like a biological phospholipid in that it had a polar head group and a nonpolar tail.

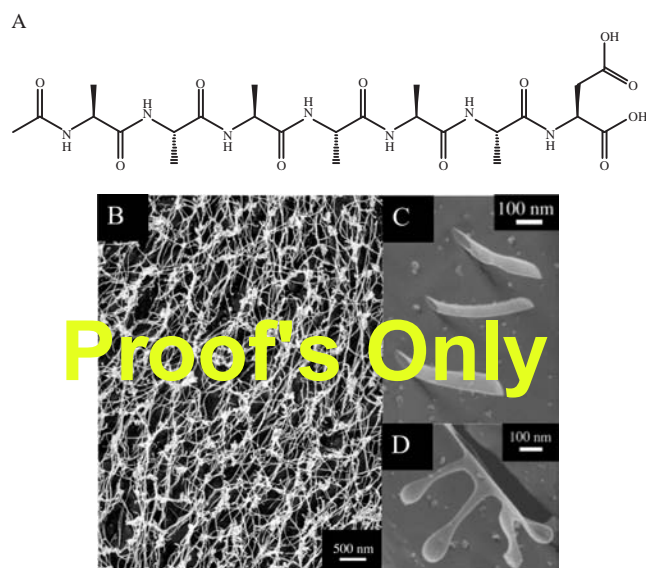


Figure 3. (A) Short surfactant-like peptide A_6D , consisting of six hydrophobic alanine amino acids followed by one negatively charged aspartic acid. (B) The nanotubes formed when this peptide was resuspended in water at pH 7. (C) Picture of V_6D peptide solution showing the presence of tubular structures. (D) V_6D solution showing vesicles budding out.

Dynamic light-scattering experiments on such small peptides in aqueous solution revealed the presence of a uniform assembly that was substantially larger than the size of individual monomers. The homogeneity and size of the supramolecular assembly were sequence-sensitive: peptides of the same length behaved differently when they had different polar head or hydrophobic tail sequences. Such phenomena have been described theoretically and experimentally in other amphiphilic systems. The shape and size of the assemblies are ultimately dependent on the size and geometry of their constituents [14].

In order to visualize the structures in solution, we utilized the transmission electron microscope (TEM). We used the quick-freeze/deep-etch method for sample preparation [17] to preserve the structures that formed in solution for electron microscopy. Each peptide solution was flash-frozen in liquid propane to prevent the formation of ice crystals. One hundred nanometers of vitreous ice were then sublimed, and the sample was coated with a 1-nm-thick platinum layer and a 20-nm-thick carbon coating and visualized using the TEM.

We observed discrete nanotubes and vesicles in the samples that gave homogeneous size distribution in the dynamic light scattering experiment (Figures 3B and 3C). Those samples that were polydispersed tended to give irregular membranous layers. The nanotubes that formed had an average diameter of around 30 nanometers as examined by TEM, consistent with results obtained from the dynamic light scattering. We also observed vesicles budding out of or fusing into a nanotube, suggesting the existence of a dynamic behavior between the different structures in the surfactant peptide system (Figure 3D).

These nanotubes have the potential to act as templates for metallization and formation of nanowires. Furthermore, the nanovesicles may be useful as an encapsulating system for drug delivery. Chemical modification of the peptide monomer may expand the function of these structures: for example, a specific cell-surface ligand can be directly incorporated into a vesicle for targeted delivery of insoluble drugs to particular cells. Current research focuses on these applications, along with more detailed structural studies and modeling of the nanostructures.

2.3.2. Cyclic Peptides with Alternating D- and L-Amino Acids

A prime example of how researchers have applied structural information of biomolecules into designing and characterizing a novel nanobiomaterial is the recent development of nanotube arrays made from cyclic peptides. The concept was first proposed by Hassal in 1972 [18] but has only recently been realized. Through several elegant experiments, Ghadiri et al. have shown that cyclic hexa- and octa-peptides with alternating D- and L-enantiomers of amino acids can regularly stack in an anti-parallel fashion to form very regular nanotube arrays, similar to hollow disks that form long cylinders [19] (Figures 4A and 4B). More importantly, the nanotubes were formed by self-assembly of the peptide disks under particular conditions, which depended on the sequences of the peptides. For example, the initial experiment involved the octa-peptide *cyclo*[-(D-Ala-Glu-D-Ala-Gln)₂-], a ring that contained the

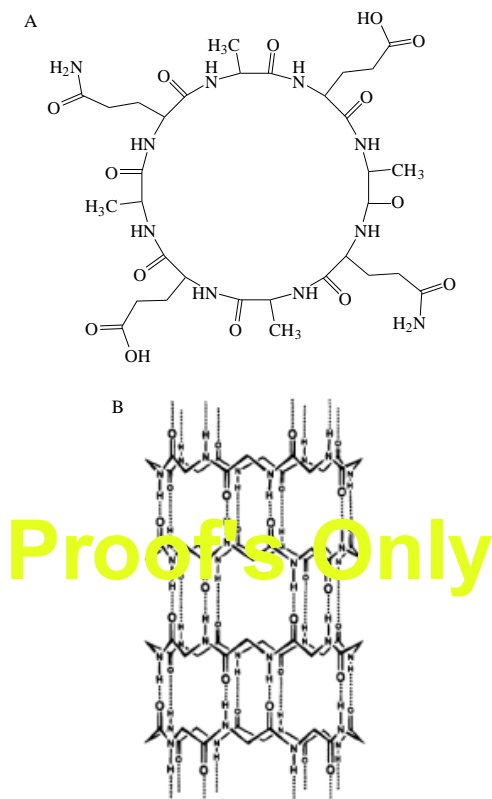


Figure 4. (A) Top-view of a *cyclo*[-(D-Ala-Glu-D-Ala-Gln)₂-] monomer, a cyclic peptide with alternating D- and L-amino acids [19]. (B) The structure of the nanotube formed by the antiparallel stacking of the cyclic peptide disks [30]. The dotted lines depict hydrogen bonding between the amide nitrogen of one disk to the amide oxygen of an adjacent disk. Reprinted with permission from [30], M. Engels et al., *J. Am. Chem. Soc.* 117, 9151 (1995). © 1995, American Chemical Society.

hydrophobic D-amino acid alanine (Ala), interspaced with either a negatively charged glutamic acid (Glu) or the polar glutamine (Gln) (Figure 4A). At neutral or alkaline pH, the glutamic acids were effectively deprotonated, and self-assembly was inhibited by electrostatic repulsion of these side chains. At lower pH values, however, the glutamic acids became protonated, the negative charges disappeared, and self-assembly occurred. Such selectivity in initiating assembly adds an important level of control for handling these nanostructures.

This cyclic peptide system has several other important properties: first, the diameter of the pore of the nanotube has the potential to be easily adjustable by changing the diameter of the peptide disk, although eight amino acid-residue peptides may be energetically preferred [20]. Second, due to the geometrical constraints imposed by the alternating amino acid enantiomers, the variable side chains of the amino acids project away from the side of the nanotubes. This is important for added functionality of the system and also for incorporation of the nanotubes into a lipid layer or a hydrophobic self-assembled monolayer (SAM).

One aspect that Ghadiri et al. investigated was the ability of these nanotubes to allow ions [21], small molecules such as glucose [22] and glutamate [23], and metal complexes of

various sizes [24] to traverse passively. With an expected pore size of 7.5 angstroms for the eight-residue peptide, ions, small organic molecules, and small metal complexes such as $K_3[Fe(CN)_6]$ and $[Ru(NH_3)_6]Cl_3$ should diffuse through, while the passage of the larger $K_4[Mo(CN)_8]$ should be hindered. For these studies, they incorporated the peptide nanotubes inside a nonpolar lipid environment [25], either in a unilamellar vesicle system or an organosulfur monolayer on gold substrates. The system allowed for a more rapid diffusion of ions than some natural systems such as gramicidin A and amphotericin B. Cyclic voltammogram experiments also revealed the size selectivity of the nanotubes. These results showed that the nanobiomaterial can serve in many applications as synthetic ion channels or as sensors for chemicals of a particular size [26, 27].

By systematically changing the sequence of the residues of the octa-peptide, Fernandez-Lopez et al. have also identified peptides that show antibacterial activity [28]. The peptide nanotube presumably increased the permeability and disrupted the integrity of the bacterial cell membrane. The sequence of the peptide affected the efficiency at which it killed a particular strain of bacteria, most likely because of specific interactions between the peptide side-chains with unique components that exist on the bacterial cell surface. This property is beneficial since inert or useful bacteria inside the body will be spared while pathogenic ones can be specifically targeted. Moreover, the peptides exerted no detrimental effects on mammalian cells, increasing their prospects to serve as antibacterial drugs.

Clark et al., in Ghadiri's laboratory, expanded the system to include nonnatural, β^3 -amino acids [29]. Through molecular modeling, the researchers proposed that these cyclic monomers should hydrogen-bond in a parallel manner to form stacked rings similar to the D, L-amino acid system. Furthermore, nanotubes made from cyclical β^3 -amino acids are expected to have a dipole moment along their lengths, which may facilitate transport of charged species.

The distinct physical parameters of the nanotubes enabled theorists and computer scientists to perform molecular dynamic studies and *ab initio* calculations of their electronic and molecular structures [30–32]. All calculations have benefited tremendously not only from previous measurements of bond angles and bond lengths of peptide molecules but also from the development of molecular dynamic software for biomacromolecules such as CHARMM [33]. Designing biologically inspired materials is facilitated by these rapid developments in molecular biology and biophysics.

2.3.3. Bolaamphiphilic Peptides

Bolaamphiphiles are amphiphilic molecules that have two hydrophilic ends joined by a hydrophobic segment. Matsui et al. investigated a peptide bolaamphiphile molecule that assembled into a nanotube at acidic pH [34]. The polymer, a bolaamphiphile that contained two glycine residues at each end and a heptane moiety at the center (Figure 5A), self-assembled into a helical ribbon at alkaline pH (Figure 5B), presumably due to the lengthening of hydrogen bonds between the carboxylic acid groups [35].

The nanotube formed was then modified in various ways. Reduction of the nanotube in nickel and copper baths yielded

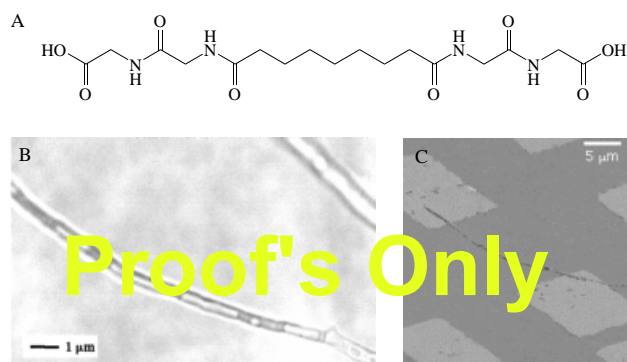


Figure 5. (A) Glycyglycine bolaamphiphile containing two glycine residues at both ends and a hydrophobic heptane group joining them [35]. (B) Tubule formed by the Bolaamphiphilic molecule at pH 4. The average diameter of the tube is 500 nm. Reprinted with permission from [35], H. Matsui and B. Gologan, *J. Phys. Chem. B* 104, 3383 (2000). © 2000, American Chemical Society. (C) A scanning electron micrograph (SEM) of a protein tubule immobilized onto biotin-SAM/Au surfaces [39]. Reproduced with permission from [39], H. Matsui et al., *Nano. Lett.* 1, 461 (2001). © 2001, American Chemical Society.

metal-amide complexes that may be used as nanowires in electrical circuits [36]. Interestingly, no metal-amide complex formed when the self-assembled structure was in the helical form, where all amide groups were hydrogen-bonded to one another. This suggested that amide hydrogen bonds are required for the formation of the complex, and that metallization will be unique to the nanotube state of this peptide system.

Nanotube immobilization on surfaces had also been achieved under two different conditions. The first condition was via hydrogen bonding to a SAM on gold surfaces [37]. The nanotube was then metallized using the aforementioned technique. The second immobilization was through specific avidin-biotin interactions [38, 39]. The nanotube was initially coated with the protein avidin, and the complex was immobilized on biotinylated SAMs. A scanning electron micrograph showed that the peptide nanotube was immobilized between two gold contacts (Figure 5C).

The experiments mentioned above are preliminary steps toward the use of biological nanotubes as construction scaffolds for nano-electronics. However, many issues remain to be resolved, such as sample heterogeneity and the effective conductivity of the metal-nanotube complex.

2.4. Peptides That Form 3-D Scaffold Hydrogels

One of the self-assembling peptide types, also called “molecular Lego,” form very stable beta-sheet structures in aqueous solution because they contain two distinct surfaces—one hydrophilic, the other hydrophobic. Like LEGO® bricks that have pegs and holes and can be assembled into particular structures at centimeter and meter scale according to a program, these peptides can do so at the nanoscale level without external instructions. The unique structural feature of these peptides is that they form complementary ionic bonds with regular repeats on the hydrophilic surface (Figure 6A). The complementary ionic sides have been classified into several

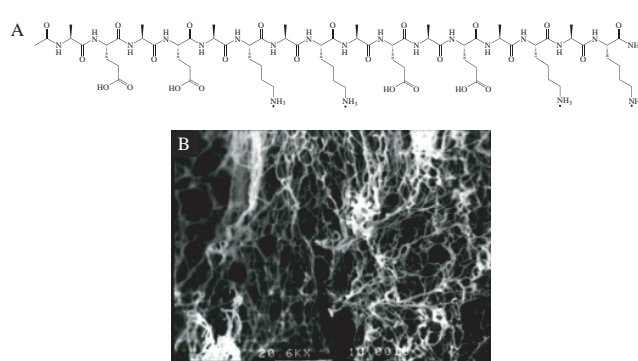


Figure 6. Self-assembling peptide to form scaffold hydrogel. (A) The sequence of the first member of the self-assembling peptides, EAK16, AEAEAKAKAEAEAKAK, serendipitously discovered in a yeast left-handed Z-DNA binding protein [74]. (B) The SEM structure revealed that the peptide self-assemble to form individual interwoven nanofibers with 50–200 nm pores. The diameter of the fiber is about 10–20 nm. Under high resolution by AFM, the filaments are revealed to be a twisted helix with regular helical repeats at early stage of self-assembly. They form scaffold hydrogel with extremely high water content (99.5–99.9%). It is likely that the nanofibers may organize water molecules.

moduli, that is, modulus I, II, III, IV, etc., and mixed moduli. This classification is based on the hydrophilic surface of the molecules that have alternating positively (+) and negatively (–) charged amino acid residues, alternating by 1, 2, 3, 4, and so on. For example, molecules of modulus I have – + – + – + – +, modulus II, – – + + – – + +, modulus IV, – – – – + + + +. These well-defined sequences allow them to undergo ordered self-assembly, resembling situation found in well-studied polymer systems.

Upon the addition of monovalent cations or the introduction of the peptide solutions into physiological media, these peptides spontaneously assemble to form macroscopic structures which can be fabricated into various geometric shapes [40, 41]. Scanning electron microscopy (SEM) and atomic force microscopy (AFM) reveal that the matrices are made of interwoven nanofibers having 10–20 nm in diameter and pores about 50–200 nm in diameter [40–45] (Figure 6B).

Atomic force microscopy and TEM experiments, as well as molecular simulation of the FKFEFKFE peptides, showed that billions of individual peptides self-assemble into nanofibers. Molecular simulation using CHARMM suggests that these individual peptides coalesce together to form a left-handed double helix with hydrophobic phenylalanines on the inside away from water, and lysines and glutamates on the outside to interact with water.

The self-assembly process is a function of time, progressing from mostly short, left-handed helical segments in the first few minutes to long nanofibers after a few hours [45]. This structure represents an example of this class of self-assembling beta-sheet peptides that spontaneously undergo association under water and physiological conditions. If the charged residues are substituted, that is, the positively charged lysines are replaced by positively charged arginines and the negatively charged glutamates are replaced by negatively charged aspartates, there are essentially no drastic effects on the self-assembly process. However, if the positively charged residues, Lys and Arg, are replaced by

negatively charged residues, Asp and Glu, the peptide can no longer undergo self-assembly to form macroscopic materials, although they can still form beta-sheet structures in the presence of salt. If the alanines are changed to more hydrophobic residues, such as Leu, Ile, Phe, or Tyr, the molecules have a greater tendency to self-assemble and form peptide matrices with enhanced strength [43–45].

Several peptide materials have been tested for their ability to support cell proliferation and differentiation. A number of mammalian cells have also been tested and all have been found to be able to form stable attachments to the peptide scaffolds [40]. These results suggested that the peptide scaffolds cannot only support various types of cell attachments, but can also allow the attached cells to proliferate and differentiate. For example, once rat PC12 cells on peptide matrices were exposed to neural growth factor (NGF), they underwent differentiation and exhibited extensive neurite outgrowth. In addition, when primary mouse neuron cells were allowed to attach the peptide materials, the neuron cells projected lengthy axons that followed the specific contours of the self-assembled peptide surface and made active and functional connections [41]. Furthermore, when chondrocytes were encapsulated in the scaffolds, the cell exhibited fully functional cartilage properties. These cells not only underwent limited proliferation, but also produced large amounts of type II and XI collagens and glycosaminoglycan, which are typical cartilage cell products [46]. This peptide scaffold is now being developed as a general three-dimensional culture system not only for a broad range of tissue cell cultures but also for tissue repair in regenerative medicine.

2.5. Peptides That Coat Surfaces

One class of peptides has been designed to self-assemble into a monolayer on surfaces and allow cells to adhere to them [47]. These peptides have three general regions along their lengths: a ligand for specific cell recognition and attachment, a linker for physical separation from the surface, and an anchor for covalent attachment to the surface (Figure 7A). The ligand may be of the RGD sequence motif that has been known to promote cell adhesion; the linker is usually a string of hydrophobic amino acids such as alanine or valine; and the anchor can be a cysteine residue for gold surfaces. Zhang et al. have used this technology in conjunction with SAMs prepared through micro-contact printing to place cells into complex patterns (Figures 7B and 7C). This approach may facilitate research into cell-cell communication.

3. NUCLEIC ACID SYSTEMS

3.1. Introduction to Nucleic Acids

Unlike proteins, nucleic acids predominantly play more inert roles in the cell. Deoxyribonucleic acid, for example, is the biopolymer that contains genetic information in its sequence and is processed and replicated by protein machineries. Even though some natural RNAs do perform enzymatic reactions and act as structural scaffolds, they are most renowned as the passive carriers of genetic information that

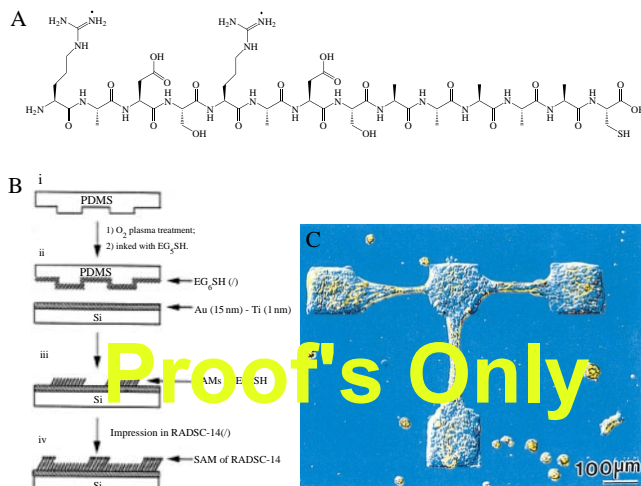


Figure 7. (A) The chemical structure of a surface-coating peptide RADSC-14 [47]; (B) a schematic diagram of micro-contact printing using RADSC-14 peptide and EG₆SH to generate a surface for cell immobilization; (C) human epidermal carcinoma cells grown on an imprinted surface. Reprinted with permission from [47], S. Zhang et al., *Biomaterials* 20, 1213 (1999). © 1999, Elsevier.

is to be translated into proteins. The simplicity of the roles of DNA and RNA, relative to proteins, is reflected in the limited number of the letters in their alphabet—four as opposed to 20 in the case of proteins. The four letters, called nucleotides, are adenine, thymine or uracil, guanine, and cytosine. Adenine is geometrically compatible with thymine, and guanine with cytosine, such that in solution, one will try to hydrogen bond to the other (Figure 8). This is called complementarity. The most ubiquitous fold that a nucleic acid

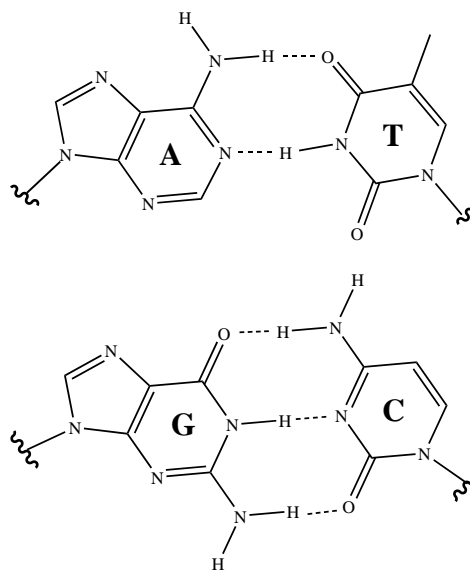


Figure 8. Chemical structure of the bases in DNA and their complementary partners. Adenine (A) form two hydrogen bonds with thymine (T), and guanine (G) form three hydrogen bonds with cytosine (C). Not pictured is the phosphate backbone of the DNA molecule that connects and arranges these bases in a spiral, ladder-like configuration.

can form is the complementary right-handed double helix, where two strands of DNA with sequences that complement each other spontaneously form an intertwining double helical structure. For example, a poly-guanine will form a double helix with a poly-cytosine. Unlike most protein folds, this structural body is utterly predictable, as one only needs to know the sequences of the two strands to predict whether a duplex will form. This ease in knowing the conformation of nucleic acids in solution has led to many ingenious experiments that manipulate DNA to perform unnatural functions, the most recent of which are entered below.

3.2. Template for Nanowire

The DNA molecule has been suggested as a template for making nanoscale wires for the emergent field of nanoelectronics. This is due to the regularity of the width of the DNA double helix and its robust mechanical properties. Several groups have succeeded in coating DNA molecules with metallic particles and have shown data on the conductive properties of these biotemplated materials.

Braun et al. noncovalently bound a stretch (16 μm) of bacteriophage λ -DNA between two gold electrodes by allowing it to hybridize with short DNA fragments that had been covalently attached to those surfaces [48]. A solution of silver ions was flowed through the self-assembled complex, allowing for the positively charged silver ions to bind to the negatively charged DNA backbone. Reduction of the silver DNA complex resulted in enlarged silver metal particles effectively coating the DNA molecule, which was confirmed using AFM.

Electrical measurements indicated that the wires were nonconducting at low voltage bias, with resistances greater than the experimentally measurable $10^{13} \Omega$. Furthermore, the shape of the I - V curve obtained was dependent on the voltage scan direction. Increasing the silver deposition reduced the severity of some of these issues, implying that modification of certain conditions may yield low-resistance metal wires which have ohmic behavior over a reasonable range of voltages.

Richter et al. employed a similar strategy to produce DNA-templated nanowires that showed relatively low resistances under low-voltage bias [49] (Figures 9A and 9B). They reduced palladium on λ -DNA and immobilized the nanowire on gold electrodes. Electron-beam-induced carbon lines were then formed between the electrodes and the ends of the nanowire, lowering the contact resistances. The resistances obtained were lower than 1 k Ω , with the specific conductivity approximately one order of magnitude lower than bulk palladium.

The resistances of these palladium nanowires were subsequently studied at low temperatures [50]. The study was performed to determine whether the biology of the material affected its behavior as a normal metal system. Theory and experiments on disordered metals showed a trend of increasing resistance with decreasing temperature at sufficiently low temperatures due to weak localization and/or enhanced electron-electron interactions. It was discovered that the palladium metals reduced on a DNA template showed the expected quantum mechanical behavior, with

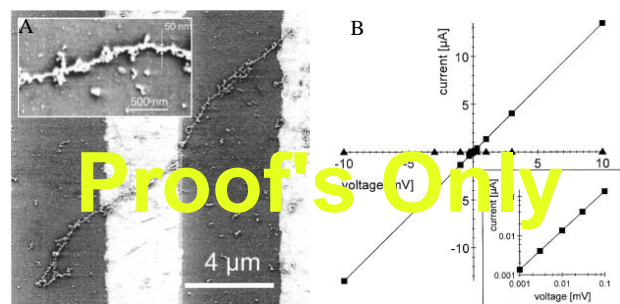


Figure 9. (A) Scanning electron micrograph of a palladium-coated λ -DNA [49]. The templated wire was laid on two gold electrodes over a SiO_2 substrate. (B) I - V curve of the wire in figure A. The inset shows the ohmic behavior of the wire down to 1 μV . Reprinted with permission from [49], J. Richter et al., *Appl. Phys. Lett.* 78, 536 (2001). © 2001, American Institute of Physics.

their resistances increasing at low temperatures. This behavior is similar to that of thin palladium films and shows that wires templated with DNA molecules behave normally.

By using first-principle molecular dynamics (FPMD), Mertig et al. discovered conditions in which fine and regular platinum clusters formed on DNA molecules [51]. They hypothesized that the rate of metal formation upon reduction of the DNA-metal ion complex depends on the number of metal nucleation events. Furthermore, this rate-limiting nucleation was controlled by Pt(II)-DNA formation during an activation step when platinum ions bound electrostatically to DNA molecules. Lengthening the activation step resulted in higher occupancy of platinum molecules in the DNA prior to reduction, and ultimately yielded a faster rate of growth and finer metal clusters on the template.

Another metal that has been investigated for surface templating of DNA is gold. Harnack et al. investigated the binding and reduction of tris(hydroxymethyl)phosphine-derivitized gold particles on calf-thymus DNA [52]. The rapidly formed nanowires show electrical conductivities about 1/1000th that of gold, which the authors attributed to the graininess of the material.

Patolsky et al. modified N -hydroxysuccinimide-gold nanoparticles with a nucleic-acid intercalating agent, amino psoralen [53]. Addition of this complex with poly-adenine/poly-thymine DNA double-strand resulted in the intercalation of gold nanoparticles to the DNA. Subsequent UV-irradiation covalently cross-linked the two species. Interestingly, deposition of the nanowires onto a mica surface resulted in their structural alignment. Even though electrical studies of these complexes were not performed, the authors showed how they utilized chemical knowledge of a biological system to engineer a desired nanostructure.

3.3. Self-Assembly Into Geometrical Objects

Designing higher-ordered structures such as a polyhedron and other geometrical objects from defined biological building blocks requires the perfect understanding of the behavior of those building blocks. Nucleic acid, in this sense, is the perfect candidate since, as mentioned previously, designing and predicting the complementarity of two nucleic acid strands is trivial. Seeman's group has intelligently designed

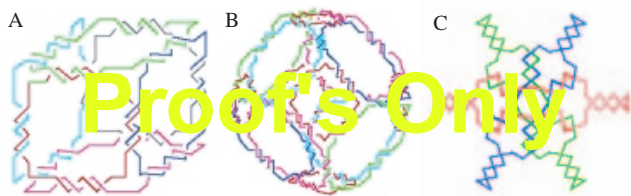


Figure 10. Geometrical objects built with DNA [75]. Pictured are schematics of (A) a cube [55]; (B) a truncated octahedron [56]; (C) a Borromean ring [57]. Reprinted with permission from [75], N. C. Seeman, *Trends in Biotechnology* 17, 437 (1999). © 1999, Elsevier Science.

a quadrilateral [54], a cube [55], a truncated octahedron [56], and Borromean rings [57] made of DNA by using a solid support system [58] (Figures 10A, 10B, and 10C, respectively). Not only did they use the knowledge they have of nucleic acids, but they also employed commonly used nucleic acid modification enzymes to build and analyze the supramolecular objects they designed.

3.4. Formation of DNA Crystal Tiles

Winfree et al. designed a set of Wang tiles made of double-crossover DNA complexes that self-assembled in solution to form macroscopic crystals [59] (Figures 11A, 11B, and 11C). The anti-parallel, double-crossover motif provides structural rigidity and predictability and was inspired by the four-way

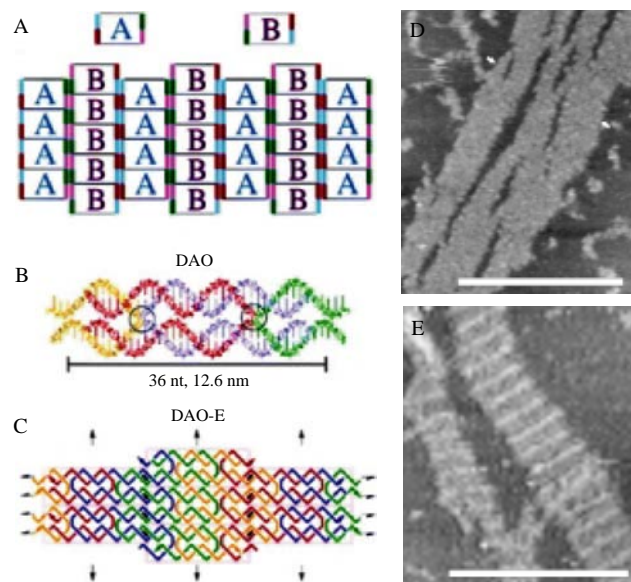


Figure 11. (A) A 2D DNA lattice made up of two Wang tiles, labeled A and B [59]. One side of the A DNA tile had sequences that matched one side of the B tile; (B) a molecular model of a tile. Each colored piece corresponds to one DNA strand; (C) the lattice topology of the assembled tiles. Black arrows indicate dyad symmetry axes; (D) AFM images of two-unit lattice as above. Scale bar corresponds to 300 nm; (E) lattice that incorporated a tile with a protruding DNA hairpin. Reprinted with permission from [59], E. Winfree et al., *Nature* 394, 539 (1998). © 1998, MacMillan Magazines Ltd.

Holliday junction structure found during meiosis, a biological process that produces the specific chromosome count in eggs and sperm. These mesoscopic tile structures grew to be as large as $2 \times 8 \mu\text{m}$ in size, with thickness that of a single tile of DNA. Each tile has the approximate size of $2 \times 4 \times 13 \text{ nm}$ and can be associated with one another through “sticky-end” ligation (hybridization and subsequent covalent linkage of complementary sequences between the DNA tiles).

Atomic force microscope images and Fourier analysis showed the presence of two-dimensional sheets with numerous column widths of 13 nm (Figure 11D), consistent with the width of a single DNA tile. Decorating one set of tiles in the two-tile system with two DNA hairpin sequences revealed this columnar structure further in the AFM, since the two hairpins protruded out and provided contrasting height with the rest of the sheet (Figure 11E). The authors also decorated the sheet with nanogold-streptavidin by incorporating a biotin moiety to the 5' end of one set of the double-crossover DNA tile.

3.5. DNA Molecular Machine

Nanometer-sized molecular “machines” based on DNA, which can cycle through different states, have also been designed. Yurke et al. designed a system, which consisted of three DNA molecules that hybridized to form a complex that could accept an incoming “fuel strand” made of another DNA molecule [60] (Figure 12A). The fluorescent quenching between two dyes on one strand (strand A in the figure) was monitored and served as an indication of the state of the system. Briefly, in an open state the two fluorescent dyes were separated such that quenching was lessened. Upon addition of a fuel strand (strand F), the system became “closed” and the two dyes were located in proximity with one another, causing quenching. Addition of a “removal strand,” \bar{F} , which was complementary to the fuel

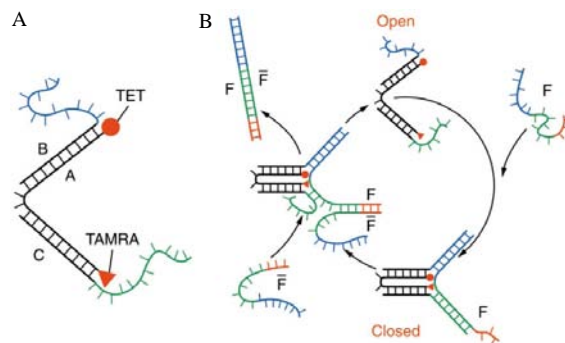


Figure 12. (A) Three strands of DNA that assembled to form the open state of a molecular tweezer [60]. TET and TAMRA are two fluorescent dyes that were attached to the ends of strand A and act as a signal of the state of the system. (B) A schematic showing the operation of the DNA-fueled molecular machine. Addition of fuel strand F closed the system and placed the two fluorescent dyes in proximity to one another, causing fluorescent quenching. The system was reset by adding the release strand, \bar{F} , which hybridized to the fuel strand. Reprinted with permission from [60], B. Yurke et al., *Nature* 406, 605 (2000). © 2000, MacMillan Magazines Ltd.

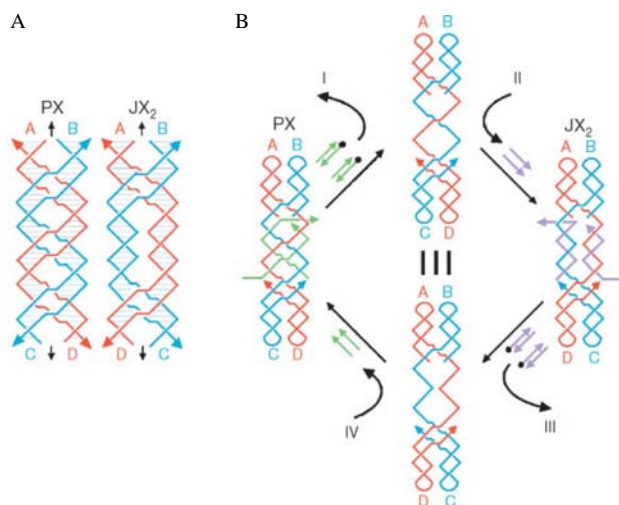


Figure 13. (A) Schematic diagram of the two topological states of a DNA machine designed by Yan et al. [61]. The black arrows indicate a central dyad axis that separates the two helical domains. The arrowheads at the end of the strands indicate the 3'-end of the DNA molecules. (B) Operation of the device. A green set strand in the PX molecule could be removed with the addition of a biotinylated complementary fuel strand, resulting in an unstructured intermediate. The intermediate can be converted into the JX₂ or back to the PX molecule by adding the appropriate set strand. Reprinted with permission from [61], H. Yan et al., *Nature* 415, 62 (2002). © 2002, MacMillan Magazines Ltd.

strand, reset the system back to the open state and generated a double-stranded DNA waste product. The cycle could then be repeated (Figure 12B).

Another system built by Yan et al. consisted of four-stranded DNA molecules that formed two parallel double helices, joined together by the crossing over of the strands [61]. This complex could adopt two stable conformations—a paranemic crossover and its topoisomer. Each was related to one another by a 180° rotation of one strand end (Figure 13A). In their scheme, Yan et al. broke apart two of the strands to make three strands (Figure 13B), the middle one called the “set” strand, and played a role in the switch between the two conformations. Addition of a “fuel” strand, which is perfectly complementary to the “set” strand, left the complex in an intermediate state. To switch the DNA machine into the other state, a different set of set strands was added which would stabilize the other conformer. Since each of these steps involved only noncovalent, hydrogen bonding between the DNA single strands, the cycle could be repeated indefinitely.

4. LIPID SYSTEM

Lipids have long been known to undergo self-assembly to form a variety of structures and colloidal materials. The traditional lipid surfactants that form nano- and micro-structural materials have penetrated into a diversity of applications, from lubricate, detergents, surface-coating to encapsulation for deliveries. The size of individual phospholipid molecules is approximately 2.5 nm in length, but they can self-assemble into millimeter-size lipid tubules with defined helical twists, many million times larger.

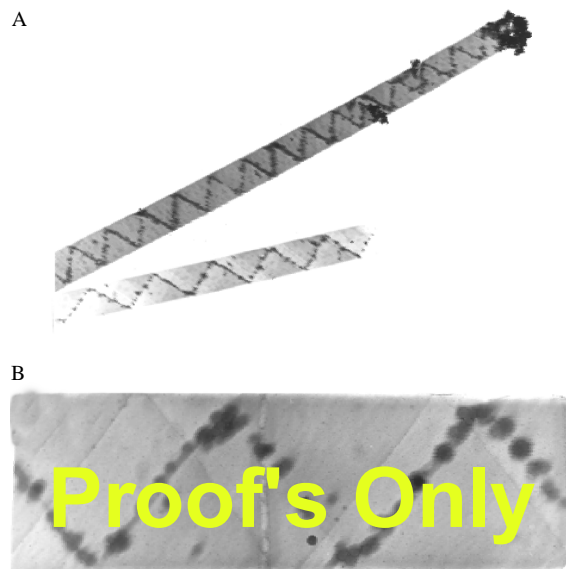


Figure 14. (A) Alignment of nanoparticles along helical ridges inside the 1 μm lipid tubules [66]. (A) magnification at 5000 \times ; (B) part of the tubule at 50,000 \times magnification. Reprinted with permission from [66], Y. M. Lvov et al., *Langmuir* 16, 5932 (2000). © 2000, American Chemical Society.

Schnur et al. have not only developed an elegant theory to explain the self-assembly of the lipid tubular structures [62], but have also developed a number of applications [63, 64]. They found that the chirality of the monomers plays a key role in the tubular structural formation. Furthermore, they can finely tune the structures at the molecular level both through synthesis of derivatives and using various solvents, especially mixing different types and concentration of alcohols [65]. They coated the metal nanocrystals onto the well-formed, left-handed microhelical tubules. These crystals metal-aligned along the helical ridge on the tubules [66] (Figures 14A and 14B). They also used the metal-coated lipid tubules to coat surfaces so that the properties of the coated surfaces can be completely altered. Their pioneering and innovative research activities have inspired more and more scientists and engineers to conduct multidisciplinary research, namely, to use biological scaffold to construct nanodevices [63].

5. BIOLOGICAL SELECTION OF PEPTIDES

5.1. Phage Display for Generating Peptides with Novel Properties

5.1.1. Peptides that Specifically Bind to Inorganic Surfaces

For particular applications that have no known analog in biology, molecular design may not be an efficient route to pursue. Even though one can potentially test many different biomolecular species to perform a particular function, the sheer number of samples that must be screened makes such an endeavor prohibitive in cost. This has led

Belcher's research group to modify an established method called phage display to generate new peptides that can selectively bind to semiconductors.

Whaley et al. started with a random library of 12 amino acid peptides that were fused to the coat protein of M13 bacteriophage (bacterial virus), resulting in one phage displaying one particular sequence of peptide [67]. The DNA that encoded for the peptide was fused with the DNA of the coat protein; sequence determination of the peptide could then be carried out by standard nucleotide sequencing of this stretch of DNA. They proceeded to allow some 10^9 phages bind to different crystalline semiconductor surfaces such as GaAs (100), GaAs (111), InP (100), and Si (100). Any phage that did not bind to the surfaces was washed away, and those that did were eluted, amplified, and re-acted under more stringent binding conditions. The process was repeated five times, yielding an exponential enrichment of those phages that displayed peptides which enabled them to bind to these inorganic surfaces.

For binding to GaAs (100), peptides with a higher number of uncharged polar and Lewis-base side-chains became more predominant with successive rounds of selection. This could be attributed to the interaction of these functional groups to the Lewis-acid sites of the GaAs surface. Furthermore, phages that bound to one particular surface showed poor binding to other surfaces, indicating that the binding was sequence-specific (Figure 15B).

5.1.2. Peptides that Bind to ZnS/Ordering of Quantum Dots

Using a similar selection strategy, Lee et al. identified a bacteriophage that had the propensity to bind to ZnS crystal surfaces (Figure 15A) [68]. These phages were then mixed with ZnS quantum dots, forming a liquid crystalline suspension of the complex. Differential interference contrast imaging and AFM studies of this suspension revealed the ordering of the bacteriophages, most likely due to the geometrical constraints of the phage body, not the attached quantum dot.

Transparent films from a suspension of viral-quantum dot assembly were made and their properties analyzed. It was discovered that the system self-assembled into a smectic-like lamellar layer, with the ZnS quantum dots localized in the region where lamellar layers met (Figures 15C and 15D). Understanding how this self-assembly occurs when the suspension is dried into a film will enable researchers to design various three-dimensional arrangements of inorganic crystals. This will push forward the areas of nano-electronic, optical, and magnetic sciences and engineering.

5.2. Artificial Peptide and Protein Libraries

Artificial peptide and protein libraries have been constructed for selection of novel proteins and peptide motifs that nature never made [69–73]. Many investigators completely designed the peptide and protein libraries *de novo*, without pre-existing protein basis. The idea of constructing protein libraries is for several reasons:

1. to further explore the enormous diversity of protein species,

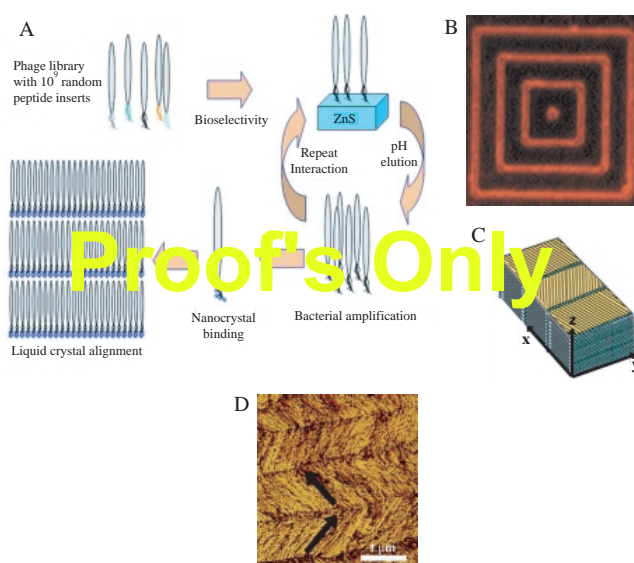


Figure 15. (A) The process employed to select phage presenting a peptide that can selectively bind to ZnS surface [68]. Reprinted with permission from [68], S. W. Lee et al., *Science* 296, 892 (2002). © 2002, American Association for the Advancement of Science. (B) Fluorescently labeled phage that specifically binds to GaAs. The surface consisted of 1 μm GaAs lines and 4 μm SiO₂ spaces [67]. Reprinted with permission from [67], S. R. Whaley et al., *Nature* 405, 665 (2000). © 2000, MacMillan Magazines Ltd. (C) Schematic drawing of the assembly of phage-bound ZnS quantum dots into a film. Reprinted with permission from [68], S. W. Lee et al., *Science* 296, 892 (2002). © 2002, American Association for the Advancement of Science. (D) AFM image of the free surface of the phage-ZnS film. Reprinted with permission from [68], S. W. Lee et al., *Science* 296, 892 (2002). © 2002, American Association for the Advancement of Science.

2. to select for a particular interesting species for a defined purpose,
3. to study protein-folding and interactions,
4. to expand knowledge of biochemistry and life forms,
5. to go beyond biology into materials sciences, molecular engineering, nanotechnology, and uncharted frontiers.

Although nature has selected and evolved many diverse proteins for all sorts of functions that support life, it has not ventured into the functions outside of life. The protein universe is enormous, in comparison with what we know today. There are, undoubtedly, a great number of more proteins that can exist beyond what has been founded in living systems.

Numerous new proteins and peptides with desired and novel properties have been selected for a particular application. This strategy permits us to purposely select and rapidly evolve nonnatural materials, nano-scaffolds, and nano-construction motifs for a growing demand in nanotechnology. The numbers of these biologically based scaffolds are limitless and they will likely play an increasingly important role for design molecular machines, nanodevices, and countless other novel, unanticipated new tools and applications.

6. SUMMARY

In this article, we summarized how different research groups have utilized the self-assembling properties of some biological molecules to form nano-materials for different applications. We categorized the systems into three broad areas, following with the identity of the biopolymer and methodology of the research—designed peptide systems, designed nucleic acid systems, and phage display (*in vivo* evolution). Each system carries distinct advantages over the others. Nucleic acids, for example, exhibit predictability in simple molecular associations. While this increases the ease of designing particular types of structures (such as sheets), it may prohibit the formation of others (such as three-dimensional gels or large nanotubes). Peptides form different nanostructures, but their self-assembling behavior is more complex, has larger degrees of freedom, and is not so well understood. Nevertheless, the different research groups have made headway in assembling different biopolymers into nano- and meso-scale structures and are starting to optimize and make modifications to them.

It is likely that these designed molecular construction motifs and nanoscale materials will become an integral part of future technology for both anticipated applications and even more importantly, unanticipated discoveries.

GLOSSARY

ACKNOWLEDGMENTS

We gratefully acknowledge the grant support from the U.S. Army Research Office, Office of Naval Research, Defense Advanced Research Project Agency/Naval Research Laboratories, and NSF CCR-0122419 to Massachusetts Institute of Technology Media Lab's Center for Bits & Atoms, National Institute of Health, Du Pont-MIT Alliance, and the Whitaker Foundation. We also gratefully acknowledge the generous educational donation of a computer cluster from the Intel Corporation.

REFERENCES

1. E. L. Chaikof, H. Matthew, J. Kohn, A. G. Mikos, G. D. Prestwich, and C. M. Yip, *Ann. N. Y. Acad. Sci.* 961, 96 (2002).
2. D. W. Hutmacher, *J. Biomater. Sci. Polym. Ed.* 12, 107 (2001).
3. L. G. Griffith and G. Naughton, *Science* 295, 1009 (2002).
4. K. E. Drexler, "Nanosystems: Molecular Machinery, Manufacturing, and Computation." Wiley, New York, 1992.
5. J. M. Gosline, P. A. Guerette, C. S. Ortlepp, and K. N. Savage, *J. Exp. Biol.* 202 Pt 23, 3295 (1999).
6. K. E. Kaissling, *Chem. Senses* 21, 257 (1996).
7. J. M. Benyus, "Biomimicry: Innovation Inspired by Nature," 1st ed. Morrow, New York, 1997.
8. M. M. Yusupov, G. Z. Yusupova, A. Baucom, K. Lieberman, T. N. Earnest, J. H. Cate, and H. F. Noller, *Science* 292, 883 (2001).
9. G. M. Whitesides and B. Grzybowski, *Science* 295, 2418 (2002).
10. C. C. Lee, J. A. Pearlman, J. S. Chamberlain, and C. T. Caskey, *Nature* 349, 334 (1991).
11. J. D. Hartgerink, E. Beniash, and S. I. Stupp, *Proc. Natl. Acad. Sci. U.S.A.* 99, 5133 (2002).
12. J. D. Hartgerink, E. Beniash, and S. I. Stupp, *Science* 294, 1684 (2001).
13. S. Weiner and H. D. Wagner, *Ann. Rev. Mater. Sci.* 28, 271 (1998).
14. J. N. Israelachvili, "Intermolecular and Surface Forces," 2nd ed. Academic Press, San Diego, 1991.
15. S. Vauthey, S. Santoso, H. Gong, N. Watson, and S. Zhang, *Proc. Natl. Acad. Sci. U.S.A.* 99, 5355 (2002).
16. S. Santoso, W. Hwang, H. Hartman, and S. G. Zhang, *Nano. Lett.* 2, 687 (2002).
17. J. Heuser, *Meth. Cell. Biol.* 22, 97 (1981).
18. C. H. Hassall (Ed.). "Proceedings of the Third American Peptide Symposium," Ann Arbor Science, 1972.
19. M. R. Ghadiri, J. R. Granja, R. A. Milligan, D. E. McRee, and N. Khazanovich, *Nature* 366, 324 (1993).
20. J. P. Lewis, N. H. Pawley, and O. F. Sankey, *J. Phys. Chem. B* 101, 10576 (1997).
21. M. R. Ghadiri, J. R. Granja, and L. K. Buehler, *Nature* 369, 301 (1994).
22. J. R. Granja and M. R. Ghadiri, *J. Am. Chem. Soc.* 116, 10785 (1994).
23. J. Sanchez-Quesada, H. S. Kim, and M. R. Ghadiri, *Angew. Chem. Internat. Ed.* 40, 2503 (2001).
24. K. Moteshareei and M. R. Ghadiri, *J. Am. Chem. Soc.* 120, 1347 (1998).
25. H. S. Kim, J. D. Hartgerink, and M. R. Ghadiri, *J. Am. Chem. Soc.* 120, 4417 (1998).
26. K. Moteshareei and M. R. Ghadiri, "Abstracts of Papers of the American Chemical Society" 213, 375 (1997).
27. J. Sanchez-Ouesada, M. P. Isler, and M. R. Ghadiri, *J. Am. Chem. Soc.* 124, 10004 (2002).
28. S. Fernandez-Lopez, H. S. Kim, E. C. Choi, M. Delgado, J. R. Granja, A. Khasanov, K. Kraehenbuehl, G. Long, D. A. Weinberger, K. M. Wilcoxon, and M. R. Ghadiri, *Nature* 412, 452 (2001).
29. T. D. Clark, L. K. Buehler, and M. R. Ghadiri, *J. Am. Chem. Soc.* 120, 651 (1998).
30. M. Engels, D. Bashford, and M. R. Ghadiri, *J. Am. Chem. Soc.* 117, 9151 (1995).
31. M. R. Ghadiri, K. Kobayashi, J. R. Granja, R. K. Chadha, and D. E. McRee, *Angew. Chem. Internat. Ed.* 34, 93 (1995).
32. D. Bashford, M. Engels, and M. R. Ghadiri, "Abstracts of Papers of the American Chemical Society" 212, 323-PHYS (1996).
33. B. R. Brooks, R. E. Brucoleri, B. D. Olafson, D. J. States, S. Swaminathan, and M. Karplus, *J. Comput. Chem.* 4, 187 (1983).
34. M. Kogiso, S. Ohnishi, K. Yase, M. Masuda, and T. Shimizu, *Langmuir* 14, 4978 (1998).
35. H. Matsui and B. Gologan, *J. Phys. Chem. B* 104, 3383 (2000).
36. H. Matsui, S. Pan, B. Gologan, and S. H. Jonas, *J. Phys. Chem. B* 104, 9576 (2000).
37. H. Matsui, B. Gologan, S. Pan, and G. E. Douberly, *Eur. Phys. J. D* 16, 403 (2001).
38. G. E. Douberly, S. Pan, D. Walters, and H. Matsui, *J. Phys. Chem. B* 105, 7612 (2001).
39. H. Matsui, P. Porrata, and G. E. Douberly, *Nano. Lett.* 1, 461 (2001).
40. S. Zhang, T. C. Holmes, C. M. DiPersio, R. O. Hynes, X. Su, and A. Rich, *Biomaterials* 16, 1385 (1995).
41. T. C. Holmes, S. de Lacalle, X. Su, G. Liu, A. Rich, and S. Zhang, *Proc. Natl. Acad. Sci. U.S.A.* 97, 6728 (2000).
42. S. Zhang, T. Holmes, C. Lockshin, and A. Rich, *Proc. Natl. Acad. Sci. U.S.A.* 90, 3334 (1993).
43. M. R. Caplan, P. N. Moore, S. Zhang, R. D. Kamm, and D. A. Lauffenburger, *Biomacromolecules* 1, 627 (2000).
44. E. J. Leon, N. Verma, S. G. Zhang, D. A. Lauffenburger, and R. D. Kamm, *J. Biomater. Sci.-Polymer Ed.* 9, 297 (1998).
45. D. M. Marini, W. Hwang, D. A. Lauffenburger, S. G. Zhang, and R. D. Kamm, *Nano. Lett.* 2, 295 (2002).
46. J. Kisiday, M. Jin, B. Kurz, H. Hung, C. Semino, S. Zhang, and A. J. Grodzinsky, *Proc. Natl. Acad. Sci. U.S.A.* 99, 9996 (2002).

47. S. Zhang, L. Yan, M. Altman, M. Lasse, H. Nugent, F. Frankel, D. A. Lauffenburger, G. M. Whitesides, and A. Rich, *Biomaterials* 20, 1213 (1999).
48. E. Braun, Y. Eichen, U. Sivan, and G. Ben-Yoseph, *Nature* 391, 775 (1998).
49. J. Richter, M. Mertig, W. Pompe, I. Monch, and H. K. Schackert, *Appl. Phys. Lett.* 78, 536 (2001).
50. J. Richter, M. Mertig, W. Pompe, and H. Vinzelberg, *Appl. Phys. A Mater. Sci. Proc.* 74, 725 (2002).
51. M. Mertig, L. C. Ciacchi, R. Seidel, W. Pompe, and A. De Vita, *Nano. Lett.* 2, 841 (2002).
52. O. Harnack, W. E. Ford, A. Yasuda, and J. M. Wessels, *Nano. Lett.* 2, 919 (2002).
53. F. Patolsky, Y. Weizmann, O. Lioubashevski, and I. Willner, *Angew. Chem. Internat. Ed.* 41, 2323 (2002).
54. J. H. Chen, N. R. Kallenbach, and N. C. Seeman, *J. Am. Chem. Soc.* 111, 6402 (1989).
55. J. H. Chen and N. C. Seeman, *Nature* 350, 631 (1991).
56. Y. W. Zhang and N. C. Seeman, *J. Am. Chem. Soc.* 116, 1661 (1994).
57. C. Mao, W. Sun, and N. C. Seeman, *Nature* 386, 137 (1997).
58. Y. W. Zhang and N. C. Seeman, *J. Am. Chem. Soc.* 114, 2656 (1992).
59. E. Winfree, F. Liu, L. A. Wenzler, and N. C. Seeman, *Nature* 394, 539 (1998).
60. B. Yurke, A. J. Turberfield, A. P. Mills, Jr., F. C. Simmel, and J. L. Neumann, *Nature* 406, 605 (2000).
61. H. Yan, X. Zhang, Z. Shen, and N. C. Seeman, *Nature* 415, 62 (2002).
62. J. V. Selinger and J. M. Schnur, *Phys. Rev. Lett.* 71, 4091 (1993).
63. J. M. Schnur, *Science* 262, 1669 (1993).
64. M. S. Spector, K. R. K. Easwaran, G. Jyothi, J. V. Selinger, A. Singh, and J. M. Schnur, *Proc. Nat. Acad. Sci. USA* 93, 12943 (1996).
65. M. S. Spector, J. V. Selinger, and J. M. Schnur, *J. Am. Chem. Soc.* 119, 8533 (1997).
66. Y. M. Lvov, R. R. Price, J. V. Selinger, A. Singh, M. S. Spector, and J. M. Schnur, *Langmuir* 16, 5932 (2000).
67. S. R. Whaley, D. S. English, E. L. Hu, P. F. Barbara, and A. M. Belcher, *Nature* 405, 665 (2000).
68. S. W. Lee, C. Mao, C. E. Flynn, and A. M. Belcher, *Science* 296, 892 (2002).
69. A. A. Furka, *Drug Discov. Today* 7, 1 (2002).
70. S. E. Blondelle and R. A. Houghten, *Trends Biotechnol.* 14, 60 (1996).
71. D. A. Moffet and M. H. Hecht, *Chem. Rev.* 101, 3191 (2001).
72. Y. Wei, T. Liu, S. L. Sazinsky, D. A. Moffet, I. Pelczer, and M. H. Hecht, *Protein Sci.* 12, 92 (2003).
73. M. Takahashi, A. Ueno, and H. Mihara, *Chemistry* 6, 3196 (2000).
74. S. Zhang, C. Lockshin, A. Herbert, E. Winter, and A. Rich, *Embo. J.* 11, 3787 (1992).
75. N. C. Seeman, *Trends in Biotechnology* 17, 437 (1999).